Noncentrosymmetric Vanadates

DOI: 10.1002/anie.200705113

The Versatile Chemistry and Noncentrosymmetric Crystal Structures of Salt-Inclusion Vanadate Hybrids**

Wendy L. Queen, J. Palmer West, Shiou-Jyh Hwu, Donald G. VanDerveer, Matthew C. Zarzyczny, and Ryan A. Pavlick*

Hybrid solids containing chemically dissimilar components have attracted much interest in advanced materials synthesis due to their structural versatility and multifunctional properties. Metal-organic frameworks (MOFs), for instance, have been extensively explored for their potential applications in technologically important fields such as heterogeneous catalysis, gas storage, and sensors.[1–3] These solids are molecule-based composite materials that contain metal ions or metal ion clusters as nodes and organic ligands as linkers. Special-framework MOFs, including noncentrosymmetric (NCS) solids, can be constructed by design due to the modular nature of their structures. Salt-inclusion solids (SISs), which are a newly emerging class of hybrid compounds, are reported to exhibit covalent metal oxide frameworks integrated with ionic lattices including alkali/alkaline-earth metal halides and others such as ammonium halides.[4–7] These all-inorganic SISs possess a fascinating structural chemistry complementary to MOFs where bonding at the interface of the dissimilar components appears to be directional. This property has been revealed through the formation of salt-templated porous frameworks[6] and NCS lattices.[7] In general, SISs are synthesized in reactive molten-salt media at 100–150 K above the melting point of the salt employed. Although no reaction mechanism has been formulated, one can imagine that the metal oxides are first "dissolved" in the corrosive molten salt and then, upon cooling, the covalent lattice aggregates around the inherent structure of the molten ionic salt[8] to form the resulting special frameworks. Employing this concept, we have recently expanded our studies in salt-inclusion chemistry into the vanadate and non-oxide systems,[9] and this is the first of several reports in the area of SISs of vanadium(V)-based mixed-metal oxides to depict the rich structural chemistry inherent in this system.

Prior to this study, most efforts in the field of salt-inclusion synthesis had been focused on creating mixed-framework solids based on transition metal (TM) phosphates, arsenates, and silicates.[4–7] Substituting the $(XO_4)^{3-}$ oxoanions (X = P, As) in the previously studied systems with the fully oxidized $(VO_4)^{3-}$ anion has allowed new structural chemistry to be unveiled. Mixing vanadium with a second TM is particularly attractive as the resulting compounds could have potential applications in areas linked to catalysis, batteries, and magnetism. This is in part due to the variable crystal chemistry of the added transition metals as well as the utility of the unique frameworks created by the salt. Structurally, like their silicate counterparts, fully oxidized vanadium(V) compounds could achieve more diversity due to their ability to form vanadate units of varying size, shape, and geometry, such as dimers, trimers, chains, and rings. Unlike Si, P, and As, however, V can adopt several different coordination modes and can therefore achieve even greater structural versatility. Furthermore, we have chosen to systematically investigate the synthesis in vanadium(V)-based systems because several V^{5+}-containing mixed-metal oxide catalysts have been reported, in energy-related studies, to be capable of splitting water into H_2 and O_2 in photocatalytic systems.[10]

Herein we report the first series of salt-inclusion vanadates, including $[(AX)_2Mn(VO_3)_2]$ (A/X = Cs/Cl (**1**), Cs/Br (**2**), and Rb/Cl (**3**)), $[(CsCl)_2Cu(VO_3)_2]$ (**4**), and $[(CsCl)Mn_2(V_2O_7)]$ (**5**). These phases adopt three distinct structures, designated as types **I** (**1**–**3**), **II** (**4**), and **III** (**5**). Compounds **1**–**3** and **5** crystallize in one of ten polar crystal classes, namely *mm*2 (C_{2v}), whereas **4** crystallizes in one of eleven nonpolar crystal classes, in this case 422 (D_4).[11] All of these acentric crystal classes have the required symmetry to lead to piezoelectric and second-harmonic generation (SHG) behaviors. The tensors for crystal class 422 nearly cancel each other out, however, and consequently the SHG measurements on a powder sample of **4** (using 1064 nm radiation)[11c] gave a doubling efficiency below the detection limit of the instrument. Compound **1** also failed to show an observable SHG response, probably due to absorption of the incident beam as a result of the sample color.

The formation of these NCS structures (Figure 1) is encouraged by structural and electronic factors. All three structure types incorporate acentric vanadate units, including metavanadate chains in **I** and **II** and pyrovanadate units in **III** (see Figures S1–S3 in the Supporting Information). Incorpo-

[*] W. L. Queen, J. P. West, Prof. S.-J. Hwu, Dr. D. G. VanDerveer, M. C. Zarzyczny
Department of Chemistry, Clemson University
Clemson, SC 29634-0973 (USA)
Fax: (+1) 864-656-6613
E-mail: shwu@clemson.edu
Homepage: http://chemistry.clemson.edu/people/hwu.htm
R. A. Pavlick
Department of Chemistry, The College of New Jersey
Ewing, NJ 08628-0718 (USA)

[**] This work was supported by the National Science Foundation (NSF) (grant nos. DMR-0322905 and 0706426). Support from the NSF for the Summer Research Program in Solid State and Materials Chemistry (for R.P.; grant no. DMR-0303450), as well as the purchase of a SQUID magnetometer and an X-ray diffractometer, are also gratefully acknowledged. The authors are indebted to Prof. P. Shiv Halasyamani and Jaewook Baek of the University of Houston for their assistance in SHG measurements and to P.S.H. for invaluable discussions.

Supporting information for this article is available on the WWW under http://www.angewandte.org or from the author.

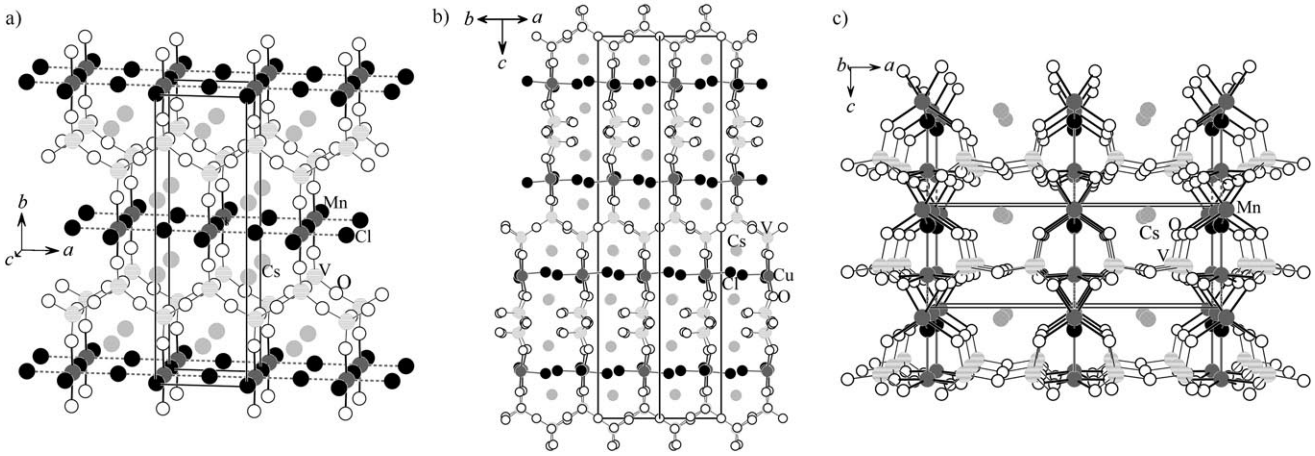

Figure 1. a) Structure of $[(CsCl)_2Mn(VO_3)_2]$ (**1**; type **I**) showing the Mn–Cl slabs interlinked by metavanadate chains. b) Projected view of $[(CsCl)_2Cu(VO_3)_2]$ (**4**; type **II**) showing the Cu–Cl sheets interlinked by nonintersecting metavanadate chains running orthogonal to one another. c) Perspective view of $[(CsCl)Mn(V_2O_7)]$ (**5**; type **III**) showing the Mn–O chains running along [010] interlinked by V_2O_7 units.

ration of a unique metavanadate chain, or pyrovanadate unit, allows the retention of the polar axis and thus the crystallization of polar compounds **1**–**3** (**I**) and **5** (**III**). Compound **4** (**II**) contains two metavanadate chains that propagate in directions orthogonal to each other, which leads to the formation of a nonpolar crystal structure. Furthermore, analysis of compounds **1**–**4** reveals that the formation of types **I** and **II** is transition metal specific (M = Mn vs. Cu; see below). The lattice in **II** compensates for the Jahn–Teller distortion found in the Cu^{2+} (d^9) ion through the formation of orthogonal metavanadate chains.

Types **I** and **II** differ with respect to the propagation directions of the metavanadate chains. Figure 1 a and b show the structures of types **I** and **II**, respectively, where single Mn–Cl and Cu–Cl sheets of the (100) ReO_3 type are interlinked by metavanadate chains. These chains propagate along the *a* direction in **I** (Figure 1 a), while in **II** they propagate in two orthogonal directions, namely the *ab* diagonals (Figure 1 b), which results in a doubling of the *c* axis. The M^{2+} cation is found in an octahedral MO_2Cl_4 geometry in both structure types. These M^{2+} cations are weakly interconnected by the Cl^- anions within the ReO_3 sheets and by an M-O-V-O-M linkage along the apex direction. The V^{5+} cation is in a tetrahedral environment and shares two corner oxygen atoms to form zigzag $(VO_3^-)_\infty$ metavanadate chains.

The metal chloride sheets contain nonuniform M–Cl bonds. Thus, the Cl atom in the structure of **1** (type **I**, Figure S4a in the Supporting Information) is not centered between two Mn atoms along the *c* axis, which results in one relatively short (2.503(1) Å) and one long (2.824(1) Å) Cl···Mn distance, although it is centered along the *a* axis to give two equally long (2.818(1) Å) Cl···Mn distances. The average Cl···Mn distance of the former pair (2.66 Å) is close to 2.64 Å, which is the sum of the Shannon crystal radii of six-coordinate Mn^{2+} (0.97 Å) and two-coordinate Cl^- (1.67 Å).[12] The structure of **4** (type **II**) contains four nonequivalent Cl···Mn distances around the Cu^{2+} center. The Cu–Cl bonds alternate along the *ab* diagonals with two short bonds of 2.279(3) and 2.288(3) Å and two long distances of 3.179(3) and 3.519(3) Å. The CuO_2Cl_4 coordination around the metal shows a tetragonal Jahn–Teller distortion. Each CuO_2Cl_2 unit, excluding the two long Cu···Cl coordination sites, is turned orthogonal with respect to its four nearest neighbors within the M–Cl slab (see Figure S4b in theSupporting Information). The bond valence sum (bvs) calculations, based on the MO_2Cl_4 polyhedra, agree with the formal oxidation states Mn^{2+} and Cu^{2+} (see Table S1 in the Supporting Information).

The size of the metal cation M also affects the structure formation. Structure type **I**, for example, shows more strain between the M–X sheet and the metavanadate chain than type **II** judging from a comparison of the O–M–O angles (160.7(1)° in **1** vs. 168.7(1)° in **4**) observed in the MO_2Cl_4 octahedral units. It is likely that the smaller Cu^{2+} cation would induce even larger strain if it were to form a structure of type **I**, and thus far the two structure types have not been found to co-exist in either compound system.

Some of the oxygen atoms in the structure of $[(RbCl)_2Mn(VO_3)_2]$ (**3**) are disordered, possibly because the smaller A-site cation causes some instability in the formation of the type **I** structure. Further experiments are underway to determine whether the potassium analogue of the Mn series forms a different structure type altogether. Also, there is experimental evidence for the existence of three additional derivatives of **4**, namely $[(KCl)_2Cu(VO_3)_2]$, $[(RbCl)_2Cu(VO_3)_2]$, and $[(CsBr)_2Cu(VO_3)_2]$ (see Figure S7 and Table S2 in the Supporting Information).

Both structure types **I** and **II** form channels: type **I** (adopted by **1**–**3**) possesses an eight-membered ring window, while type **II** (**4**) exhibits a 14-membered ring containing the cation centers of mixed MO_2X_4 and VO_4 polyhedra (see Figures S1 and S2 in the Supporting Information). The Cs and Cl ions reside in the channels of **1** and **4** at an average distance of 3.58 and 3.62 Å, respectively, as expected for a CsCl salt (3.57 Å).

Initial Li^+ cation-exchange experiments have been performed with single crystals of **1** and **4** at 60 and 200 °C using the methods reported previously.[13] The EDX results suggest that no CsCl salt remains in the solid products. Further studies

of the nature of the salt-free structures obtained are underway.

Structure type **III** adopted by $[(CsCl)Mn_2(V_2O_7)]$ (**5**) contains Mn^{2+} cations in two crystallographically distinct sites, both of which are found in highly distorted pseudo-octahedral MO_4Cl_2 geometries (Figure 2). The polyhedral

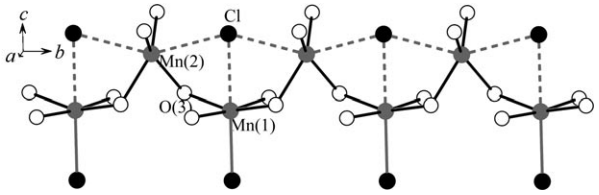

Figure 2. $[Mn_2O_6Cl_2]_\infty$ chain in the type **III** structure.

units share corner oxygen atoms along [010] to form $[Mn_2O_6Cl_2]_\infty$ chains. Parallel chains are interlinked along the *a* axis by $(V_2O_7)^{4-}$ pyrovanadate anions and along the *b* axis by a single VO_4 unit (Figure 1c and Figure S3 in the Supporting Information). The V–O–V bridging angle of the acentric V_2O_7 unit bends in a unique direction, thereby allowing the creation of a polar axis. Like types **I** and **II**, type **III** also has a channel-type structure where six-membered ring windows can be seen along all three crystallographic axes. The Cs^+ cation resides in the channel and is loosely coordinated to the Cl^- anion with a long Cs···Cl distance of 3.781(1) Å (3.57 Å in CsCl).

Finally, the NCS vanadate-based compounds **1**–**5** show three new Cl-centered acentric units (Figure 3), where Cl is off-center in a distorted octahedral coordination environment (2 Mn + 4 Cs, 2 Cu + 4 Cs, and 4 Mn + 2 Cs for types **I**—**III**,

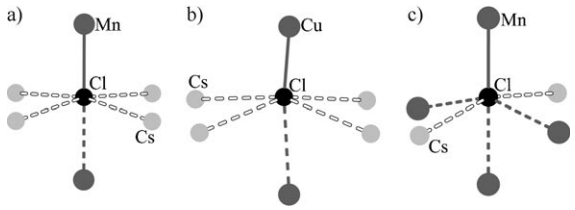

Figure 3. Cl-centered acentric units found in types **I** (a), **II** (b), and **III** (c).

respectively). Previous reports have recognized Cl-centered acentric units as playing an essential role in the formation of NCS structures. These reports include honeycomb-like channels in [BaCl]$CuPO_4$ (CU-1),[7a] irregular channel structures in two members of the $Cu_{2n-1}(P_2O_7)_n^{2-}$ series, namely $Cs_2Cu_7(P_2O_7)_4 \cdot 6\,CsCl$ (CU-9, $n = 4$) and $Cs_2Cu_5(P_2O_7)_3 \cdot 3\,CsCl$ (CU-11, $n = 3$),[7b] the fresnoite-type polar framework of $Ba_2Mn(Si_2O_7)Cl$ (CU-13),[7c] and the nonbonding-electron-directed channels in $(Ba_6Cl_3)M_{4+x}Si_{12-x}O_{34}$ (CU-14, where M = Mn, $x = 0$; M = Fe, $x = 1$).[7d,e] The acentricity of these units in the title compounds is attributed to the presence of short (solid lines in Figure 3) and long (dashed lines in Figure 3) Cl–M bonds (M = Mn and Cu) and their asymmetric arrangements in an octahedral coordination.

In conclusion, the two structure types **I** and **II** do not coexist in the $(AX)_2M(VO_3)_2$ series, which means that the structure formation is M^{2+} cation specific. It will be interesting to see whether the use of other Jahn–Teller ions can induce the exclusive formation of type **II**. Meanwhile, we have isolated many novel vanadate phases, including some containing magnetic nanostructures and open-framework networks, by varying the stoichiometry of the salts. Detailed investigations and analysis of the utility of salts in special framework formation are currently underway.

Experimental Section

The $(AX)_2M(VO_3)_2$ phases **1**–**4** were synthesized by employing stoichiometric amounts of MO (M = Mn, Cu), V_2O_5, and AX in a total mass of about 0.3 g. The reactants were heated to 600 °C, isothermed for 2 days, and then furnace-cooled. Plate-like crystals were obtained in various yields. $(CsCl)Mn_2(V_2O_7)$ (**5**) was synthesized by mixing MnO and V_2O_5 in a 1:1 molar ratio (about 0.3 g) with a CsCl/NaCl eutectic flux equal to three times the mass of the reactants. The mixture was heated to 650 °C, isothermed for 4 days, slowly cooled to 450 °C, and then furnace-cooled.

All reaction mixtures were sealed under vacuum in carbon-coated quartz ampoules. See the Supporting Information for more detailed results in terms of product distributions.

Crystal data: **1**: $(CsCl)_2Mn(VO_3)_2$, $M_r = 589.54$, orthorhombic, space group *Cmm*2 (no. 35), $a = 5.634(1)$, $b = 17.892(4)$, $c = 5.326(1)$ Å, $V = 537.0(2)$ Å^3, $Z = 2$, $\rho_{calcd} = 3.646$ g cm^{-3}, final $R = 0.0287$, $Rw = 0.0720$, GOF = 0.975 (all data), 43 parameters. **2**: $(CsBr)_2Mn(VO_3)_2$, $M_r = 678.44$, orthorhombic, space group *Cmm*2 (no. 35), $a = 5.681(1)$, $b = 17.915(4)$, $c = 5.601(1)$ Å, $V = 570.9(2)$ Å^3, $Z = 2$, $\rho_{calcd} = 3.947$ g cm^{-3}, final $R = 0.0593$, $Rw = 0.1633$, GOF = 1.071 (all data), 43 parameters. **3**: $(RbCl)_2Mn(VO_3)_2$, $M_r = 494.66$, orthorhombic, space group *Cmm*2 (no. 35), $a = 5.441(1)$, $b = 17.609(4)$, $c = 5.148(1)$ Å, $V = 493.3(2)$ Å^3, $Z = 2$, $\rho_{calcd} = 3.331$ g cm^{-3}, final $R = 0.0836$, $Rw = 0.2153$, GOF = 1.160 (all data), 50 parameters. **4**: $(CsCl)_2Cu(VO_3)_2$, $M_r = 598.14$, tetragonal, space group $P4_12_12$ (no. 92), $a = 7.915(1)$, $c = 34.664(7)$ Å, $V = 2171.7(6)$ Å^3, $Z = 8$, $\rho_{calcd} = 3.201$ g cm^{-3}, final $R = 0.0431$, $Rw = 0.1138$, GOF = 1.050 (all data), 121 parameters. **5**: $(CsCl)Mn_2(V_2O_7)$, $M_r = 589.54$, orthorhombic, space group *Pma*2 (no. 28), $a = 14.948(3)$, $b = 5.545(1)$, $c = 5.295(1)$ Å, $V = 438.8(2)$ Å^3, $Z = 2$, $\rho_{calcd} = 3.724$ g cm^{-3}, final $R = 0.0292$, $Rw = 0.0687$, GOF = 1.068 (all data), 65 parameters.

Data were collected with a four-circle Rigaku AFC8 diffractometer equipped with a Mercury CCD area detector and a $Mo_{K\alpha}$ ($\lambda = 0.71073$ Å) radiation source in the 2θ range 2.50–52.5°. Further details of the crystal structure investigations may be obtained from the Fachinformationszentrum Karlsruhe, 76344 Eggenstein-Leopoldshafen, Germany (fax: (+49) 7247-808-666; e-mail: crysdata@fiz-karlsruhe.de), on quoting the depository numbers CSD-418760–418764.

Received: November 5, 2007
Revised: February 13, 2008
Published online: April 9, 2008

Keywords: inclusion compounds · Jahn–Teller distortion · noncentrosymmetric solids · solid-state structures · vanadates

[1] S. Kitagawa, R. Kitaura, S.-I. Noro, *Angew. Chem.* **2004**, *116*, 2388–2430; *Angew. Chem. Int. Ed.* **2004**, *43*, 2334–2375.

[2] a) M. Eddaoudi, D. B. Moler, H. Li, B. Chen, T. M. Reineke, M. O'Keeffe, O. M. Yaghi, *Acc. Chem. Res.* **2001**, *34*, 319–330; b) N. W. Ockwig, O. Delgado-Friedrichs, M. O'Keeffe, O. M. Yaghi, *Acc. Chem. Res.* **2005**, *38*, 176–182.

[3] a) M. J. Rosseinsky, *Microporous Mesoporous Mater.* **2004**, *73*, 15 – 30; b) W. Lin, *MRS Bull.* **2007**, *32*, 544 – 548.
[4] a) A. Müller, H. Reuter, S. Dillinger, *Angew. Chem.* **1995**, *107*, 2505 – 2539; *Angew. Chem. Int. Ed. Engl.* **1995**, *34*, 2328 – 2361; b) R. Rettich, H. Müller-Buschbaum, *Z. Naturforsch. B* **1997**, *52*, 457 – 461; c) Q. Huang, M. Ulutagay-Kartin, X. Mo, S.-J. Hwu, *Mater. Res. Soc. Symp. Proc.* **2002**, *755*, 459 – 464; d) C.-H. Liao, P.-C. Chang, H.-M. Kao, K.-H. Lii, *Inorg. Chem.* **2005**, *44*, 9335 – 9339.
[5] a) M. Ulutagay, G. L. Schimek, S.-J. Hwu, H. Taye, *Inorg. Chem.* **1998**, *37*, 1507 – 1512; b) S.-J. Hwu, M. Ulutagay-Kartin, J. A. Clayhold, R. Mackay, T. A. Wardojo, C. J. O'Connor, M. Krawiec, *J. Am. Chem. Soc.* **2002**, *124*, 12404 – 12405.
[6] a) Q. Huang, M. Ulutagay, P. A. Michener, S.-J. Hwu, *J. Am. Chem. Soc.* **1999**, *121*, 10323 – 10326; b) Q. Huang, S.-J. Hwu, X. Mo, *Angew. Chem.* **2001**, *113*, 1754 – 1756; *Angew. Chem. Int. Ed.* **2001**, *40*, 1690 – 1693.
[7] a) K. M. S. Etheredge, S.-J. Hwu, *Inorg. Chem.* **1995**, *34*, 3123 – 3125; b) Q. Huang, S.-J. Hwu, *Inorg. Chem.* **2003**, *42*, 655 – 657; c) X. Mo, S.-J. Hwu, *Inorg. Chem.* **2003**, *42*, 3978 – 3980; d) X. Mo, E. Ferguson, S.-J. Hwu, *Inorg. Chem.* **2005**, *44*, 3121 – 3126; e) X. Mo, Ph.D. dissertation, Clemson University, **2005**.
[8] See, for example: R. A. La Violette, J. L. Budzien, F. H. Stillinger, *J. Chem. Phys.* **2000**, *112*, 8072 – 8078.
[9] a) L. Wang, Y.-C. Hung, S.-J. Hwu, H.-J. Koo, M.-H. Whangbo, *Chem. Mater.* **2006**, *18*, 1219 – 1225; b) L. Wang, S.-J. Hwu, *Chem. Mater.* **2007**, *19*, 6212 – 6221.
[10] a) H. Harada, C. Hosoki, A. Kudo, *J. Photochem. Photobiol. A* **2001**, *141*, 219 – 224; b) J. Ye, Z. Zou, M. Oshikiri, A. Matsushita, M. Shimoda, M. Imai, T. Shishido, *Chem. Phys. Lett.* **2002**, *356*, 221 – 226.
[11] a) P. S. Halasyamani, K. R. Poeppelmeier, *Chem. Mater.* **1998**, *10*, 2753 – 2769; b) P. S. Halasyamani, *Chem. Mater.* **2004**, *16*, 3586 – 3592; c) K. M. Ok, E. O. Chi, P. S. Halasyamani, *Chem. Soc. Rev.* **2006**, *35*, 710 – 717.
[12] R. D. Shannon, *Acta Crystallogr. Sect. A* **1976**, *32*, 751 – 767.
[13] G. Becht, S.-J. Hwu, *Chem. Mater.* **2006**, *18*, 4221 – 4223.

